Supporting Information

Tunable Dual White Light Emission from Gua_3CuCl_4 and $Gua_7Cu_3X_{10}\cdot 3DMF$ (X = Br, I)

*Isaiah W. Gilley, Tielyr D. Creason, Timothy M. McWhorter, Bayram Saparov**

I. W. Gilley, T. D. Creason, T. M. McWhorter, B. Saparov

Department of Chemistry and Biochemistry, University of Oklahoma, 101 Stephenson Parkway, Norman, OK 73019, United States

*Corresponding Author: saparov@ou.edu

Downloaded from SHAREOK. Persistent Handle URL: https://hdl.handle.net/11244/336539

Table S1. Selected single crystal data and structure refinement parameters for Gua_3CuCl_4 and $Gua_7Cu_3Br_{10}\cdot 3DMF$.

Formula	$(CH_6N_3)_3CuCl_4$	$(CH_6N_3)_7Cu_3Br_{10}\cdot 3(C_3H_7NO)$
Formula weight (g/mol)	385.59	1629.62
Temperature (K)	100(2)	
Radiation, wavelength (Å)	Mo Kα, 0.71073	
Crystal system	Orthorhombic	Trigonal
Space group	$Pna2_1$	$P31c$
Z	4	
Unit cell parameters (Å, °)	a = 11.5195(3) b = 10.1581(3) c = 26.3272(7) α = 90 β = 90 γ = 90	a = 14.8235(5) b = 14.8235(5) c = 14.2712(6) α = 90 β = 90 γ =120
Volume (Å^3)	3080.71(15)	2715.8(2)
Density (ρ_{calc}) (g/cm^3)	1.663	1.993
Absorption coefficient (μ) (mm^{-1})	2.107	8.567
$\theta_{min} - \theta_{max}$ (°)	2.673 – 28.750	2.134 – 30.606
Reflections collected	36927	70252
Independent reflections	7909	5574
R^a indices ($I > 2\sigma(I)$)	R_1 = 0.0302 wR_2 = 0.0798	R_1 = 0.0363 wR_2 = 0.0898
Goodness-of-fit on F^2	1.026	1.005
Largest diff. peak and hole (e$^-$/Å^3)	0.481 and -0.514	1.823 and -1.241

[a] $R_1 = \sum\left||F_0| - |F_c|\right| / \sum|F_0|$; $WR_2 = \sqrt{\sum|w(F_0^2 - F_c^2)^2| / \sum\left|wF_0^{2\,2}\right|}$,
where $w = 1/|\sigma^2 F_0^2 + (AP)^2 + BP|$, with $P = (F_0^2 + 2F_c^2)/3$ and weight coefficients A and B

Table S2. Atomic coordinates and equivalent isotropic displacement parameters (U_{eq}[a]) for Gua_3CuCl_4.

$(CH_6N_3)_3CuCl_4$				
Atom	***x***	***y***	***z***	U_{eq}, Å^2
C1	0.2799(5)	0.1312(5)	0.56396(19)	0.0243(10)
C2	0.5433(4)	0.0463(5)	0.43586(18)	0.0196(9)
C3	0.3038(5)	0.1543(5)	0.3116(2)	0.0242(10)
C4	0.6282(4)	0.8190(5)	0.31840(19)	0.0197(9)
C5	0.5576(4)	0.4978(5)	0.69266(18)	0.0188(9)
C6	0.4632(5)	0.6814(5)	0.56270(18)	0.0235(10)
N1	0.3310(5)	0.0308(5)	0.54102(19)	0.0300(10)
N2	0.3379(5)	0.1944(5)	0.60079(19)	0.0331(11)
N3	0.1742(4)	0.1673(5)	0.55199(19)	0.0293(10)
N4	0.6085(4)	-0.0616(5)	0.43820(19)	0.0268(9)
N5	0.4324(4)	0.0365(5)	0.42519(18)	0.0248(9)
N6	0.5919(4)	0.1643(4)	0.44177(18)	0.0274(9)
N7	0.2563(4)	0.2329(5)	0.34667(18)	0.0286(10)
N8	0.4071(4)	0.1823(5)	0.29235(18)	0.0259(9)
N9	0.2465(5)	0.0475(5)	0.29751(19)	0.0291(10)
N10	0.5253(4)	0.8024(5)	0.29677(18)	0.0246(9)
N11	0.6904(4)	0.9257(4)	0.30680(18)	0.0220(8)
N12	0.6674(4)	0.7325(4)	0.35200(17)	0.0238(9)
N13	0.6727(4)	0.4969(5)	0.6898(2)	0.0270(9)
N14	0.5012(4)	0.6109(5)	0.69482(18)	0.0251(9)
N15	0.5004(4)	0.3831(5)	0.69338(18)	0.0264(10)
N16	0.5614(4)	0.6949(5)	0.53653(19)	0.0307(10)
N17	0.4359(4)	0.7719(5)	0.59675(18)	0.0275(9)
N18	0.3948(5)	0.5783(5)	0.5557(2)	0.0326(11)
Cu1	0.12997(5)	0.49022(6)	0.66189(2)	0.02278(14)
Cu2	0.45685(5)	0.51245(6)	0.41532(2)	0.02283(14)
Cl1	0.10922(11)	0.47183(13)	0.57447(5)	0.0268(3)
Cl2	0.22276(10)	0.32317(11)	0.70706(5)	0.0216(2)
Cl3	0.22996(10)	0.68987(11)	0.67258(5)	0.0239(2)
Cl4	-0.04926(10)	0.51985(13)	0.70281(5)	0.0255(3)
Cl5	0.36394(10)	0.35120(11)	0.46302(5)	0.0234(2)
Cl6	0.38033(11)	0.71975(11)	0.42974(5)	0.0272(3)
Cl7	0.46475(10)	0.48422(11)	0.32705(4)	0.0219(2)
Cl8	0.65240(10)	0.49571(12)	0.44265(5)	0.0231(2)

Table S3. Atomic coordinates and equivalent isotropic displacement parameters (U_{eq}[a]) for $Gua_7Cu_3Br_{10}\cdot 3DMF$.

$(CH_6N_3)_7Cu_3Br_{10}\cdot 3DMF$

Atom	***x***	***y***	***z***	U_{eq}, **Å^2**
C1	0.6687(6)	0.6699(6)	0.5784(9)	0.0378(19)
C2	1.0046(9)	0.6284(9)	0.3177(7)	0.047(2)
C3	0.6857(12)	0.3470(15)	0.3101(8)	0.025(4)
C4	0.7076(17)	0.6419(16)	0.3287(17)	0.113(6)
C5	0.8415(17)	0.8200(19)	0.3298(17)	0.140(9)
C6	0.6516(19)	0.769(2)	0.3256(18)	0.168(11)
N1	0.7711(5)	0.7165(6)	0.5834(7)	0.042(2)
N2	0.6128(6)	0.5671(5)	0.5822(9)	0.057(3)
N3	0.6218(5)	0.7258(5)	0.5779(8)	0.045(2)
N4	1.0908(9)	0.6216(8)	0.3129(7)	0.058(3)
N5	0.9699(12)	0.6450(11)	0.2406(7)	0.075(4)
N6	0.9677(9)	0.6259(11)	0.4012(7)	0.069(3)
N7	0.726(2)	0.3694(18)	0.3952(13)	0.072(11)
N8	0.677(3)	0.265(2)	0.2653(15)	0.065(8)
N9	0.654(3)	0.406(3)	0.2697(19)	0.085(12)
N10	0.7312(10)	0.7411(11)	0.3319(10)	0.081(3)
Cu1	0.666667	0.333333	0.99012(11)	0.0248(3)
Cu2	0.666667	0.333333	0.64421(11)	0.0228(3)
Cu3	1.000000	1.000000	0.57536(16)	0.0356(4)
Br1	0.63442(5)	0.16183(6)	1.04952(5)	0.02322(17)
Br2	0.80861(5)	0.50431(5)	0.58889(5)	0.02352(18)
Br3	0.666667	0.333333	0.81848(13)	0.0501(4)
Br4	1.02747(6)	0.85527(6)	0.57222(11)	0.0488(3)

Table S4. A comparison of bond distances and angles within the polyhedral units of Gua_3CuCl_4 and $Gua_7Cu_3Br_{10}\cdot 3DMF$.

Atom pair	Distance (Å)	Atom Labels	Angle (°)
$(CH_6N_3)_3CuCl_4$			
$[CuCl_4]^{3-}$ Tetrahedral Unit			
Cu1 – Cl1	2.3216(14)	Cl1-Cu1-Cl2	119.62(5)
Cu1 – Cl2	2.3315(13)	Cl1-Cu1-Cl3	103.81(5)
Cu1 – Cl3	2.3492(13)	Cl1-Cu1-Cl4	112.00(5)
Cu1 – Cl4	2.3482(13)	Cl2-Cu1-Cl3	110.03(5)
Cu2 – Cl5	2.3142(13)	Cl2-Cu1-Cl4	105.21(5)
Cu2 – Cl6	2.3250(13)	Cl3-Cu1-Cl4	105.40(5)
Cu2 – Cl7	2.3434(13)	Cl5-Cu2-Cl6	112.15(5)
Cu2 – Cl8	2.3708(13)	Cl5-Cu2-Cl7	117.86(5)
		Cl5-Cu2-Cl8	102.88(5)
		Cl6-Cu2-Cl7	106.79(5)
		Cl6-Cu2-Cl8	112.18(5)
		Cl7-Cu2-Cl8	104.79(5)
$(CH_6N_3)_7Cu_3Br_{10}\cdot 3DMF$			
$[Cu_2Br_7]^{2-}$ Tetrahedral Unit			
Cu1 – Br1 (×3)	2.4889(9)	Br1-Cu1-Br1 (×3)	109.03(4)
Cu1 – Br3	2.450(2)	Br1-Cu1-Br3 (×3)	109.91(4)
Cu2 – Br2 (×3)	2.4781(9)	Br2-Cu2-Br2 (×3)	110.35(4)
Cu2 – Br3	2.487(2)	Br2-Cu2-Br3 (×3)	108.58(4)
$[CuBr_3]^{2-}$ Trigonal Planar Unit			
Cu3-Br4 (×3)	2.3758(8)	Br4-Cu3-Br4 (×3)	119.965(5)

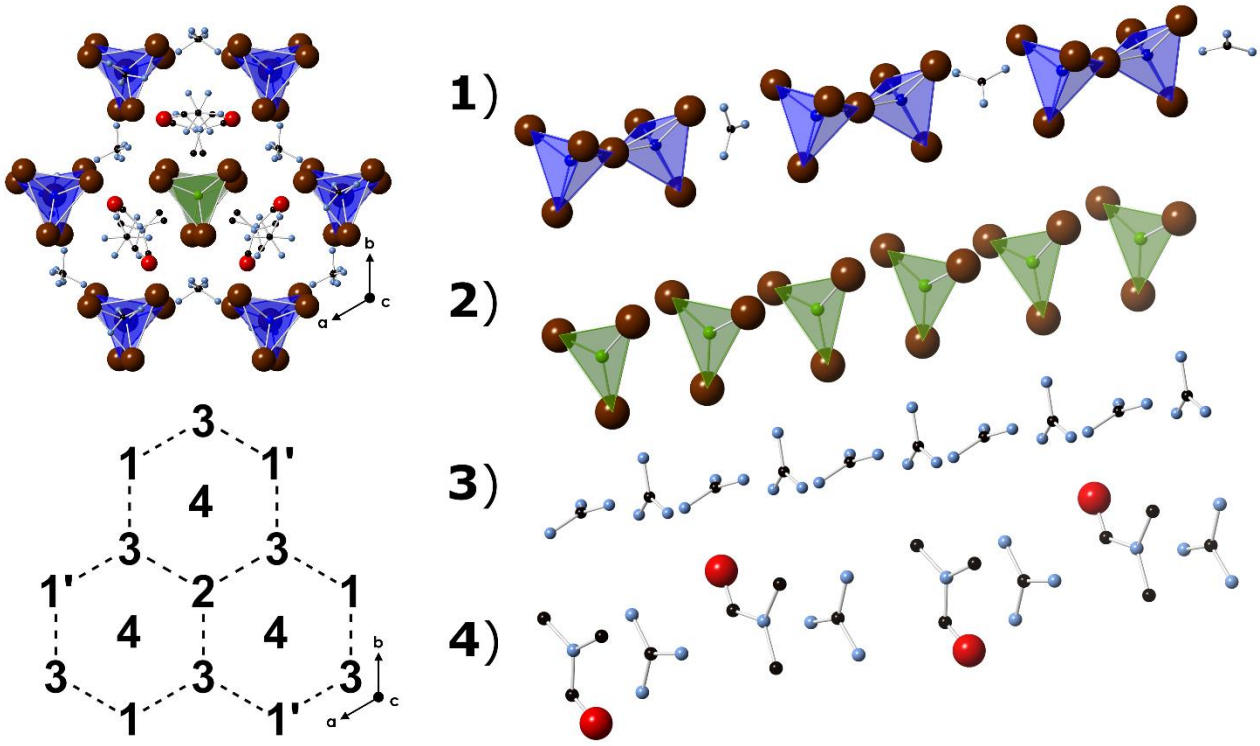


Figure S1. A polyhedral model depicting the arrangement of four pseudo-chains within the $Gua_7Cu_3Br_{10}\cdot 3DMF$ structure projected down the *c*-axis. 1) Alternating tetrahedral dimer $[CuBr_7]^{5-}$ units and guanidinium molecules, with 1` indicating chains starting from a guanidinium molecule. 2) Trigonal planar $[CuBr_3]^{2-}$ units. 3) Alternating DMF and guanidinium molecules. 4) Guanidinium molecules with alternating orientation. Tetrahedral dimer $[Cu_2Br_7]^{5-}$ units are colored in blue, trigonal planar $[CuBr_3]^{2-}$ units are colored in green, and carbon, nitrogen, oxygen, and bromine are colored black, light blue, red, and brown, respectively.

Table S5. Fitting parameters for time resolved photoluminescence of $Gua_7Cu_3Br_{10}\cdot 3DMF$ and $Gua_7Cu_3I_{10}\cdot 3DMF$.

Parameter	**$Gua_7Cu_3Br_{10}\cdot 3DMF$**	**$Gua_7Cu_3I_{10}\cdot 3DMF$**
A_0 (counts)	298 ± 4	357 ± 1
A_1	96 ± 3	1.37 ± 0.02
A_2	106 ± 2	2.100 ± 0.009
A_3	58 ± 3	
$\boldsymbol{\tau_1}$	183 ± 37 ns	28 ± 1 ns
$\boldsymbol{\tau_2}$	1.35 ± 0.34 μs	161 ± 3 ns
$\boldsymbol{\tau_3}$	49 ± 5 ns	
Average Lifetime	1.20 ± 0.31 μs	147 ± 3 ns
χ^2	0.9698455	0.9857442

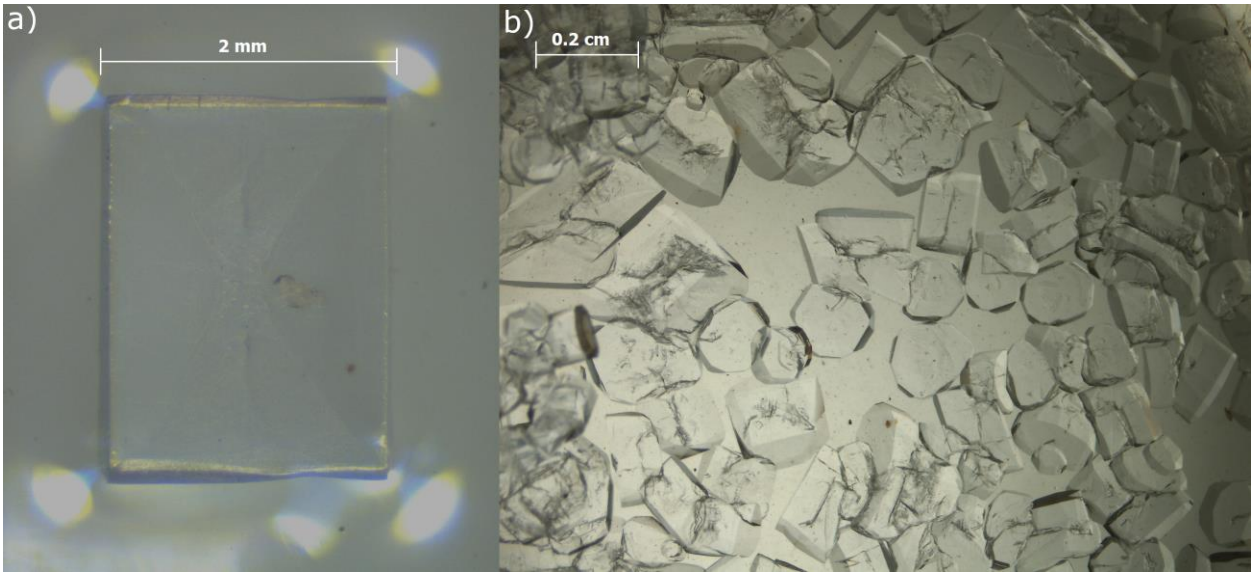


Figure S2. Photographs of $Gua_7Cu_3I_{10}\cdot 3DMF$ grown *via* slow cooling in DMF.

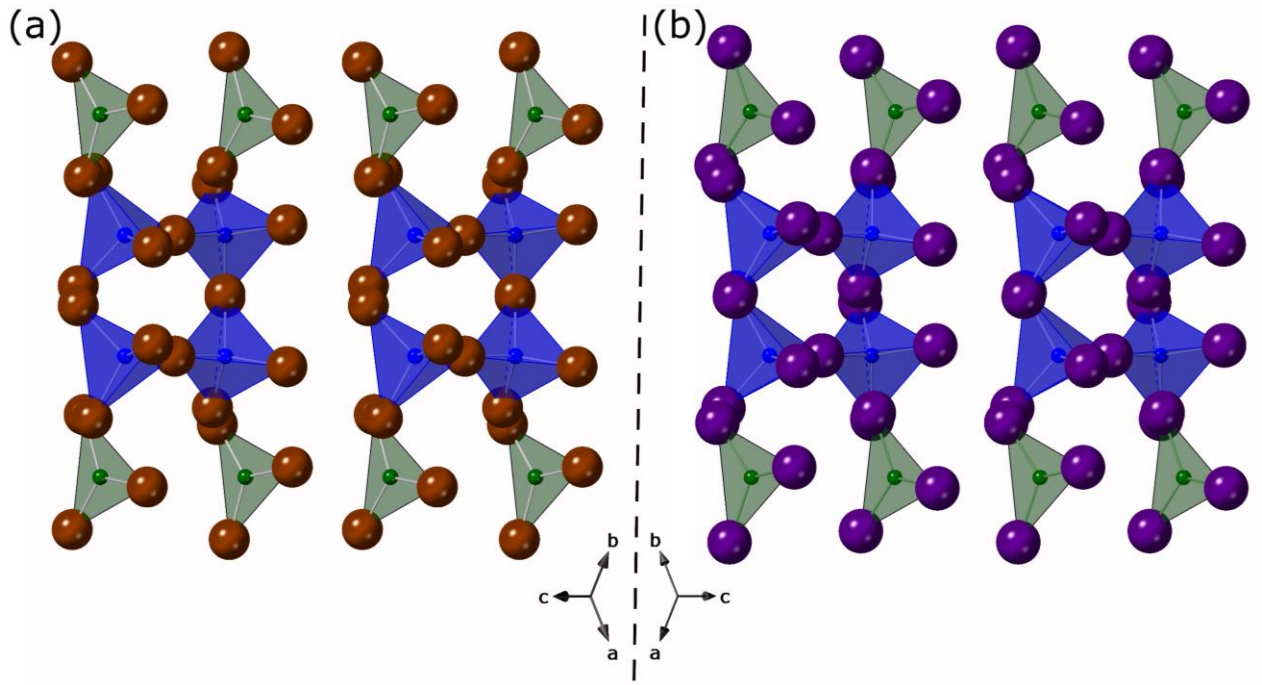


Figure S3. A comparison between polyhedral models of (a) the crystal structure of $Gua_7Cu_3Br_{10}\cdot 3DMF$ projected down the [-1-1-1] direction and (b) a partially solved structure for $Gua_7Cu_3I_{10}\cdot 3DMF$ projected down the [111] direction. Organic components have been omitted from the $Gua_7Cu_3Br_{10}\cdot 3DMF$ model to improve visual clarity. Tetrahedral dimer $[Cu_2X_7]^{5-}$ units are colored in blue, trigonal planar $[CuX_3]^{2-}$ units are colored in green, and bromine and iodine are colored brown and purple, respectively.

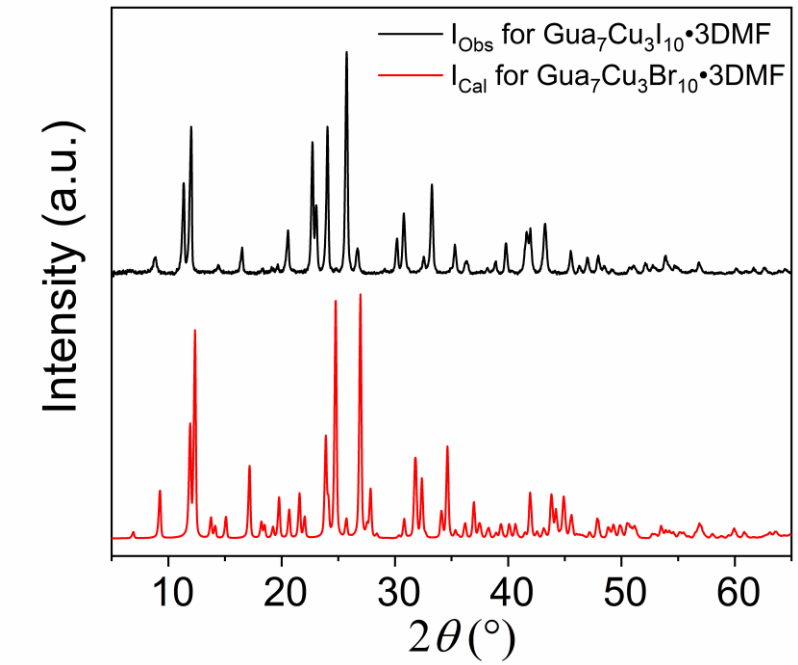


Figure S4. Comparison of the PXRD spectra of $Gua_7Cu_3Br_{10}$·3DMF and $Gua_7Cu_3I_{10}$·3DMF.

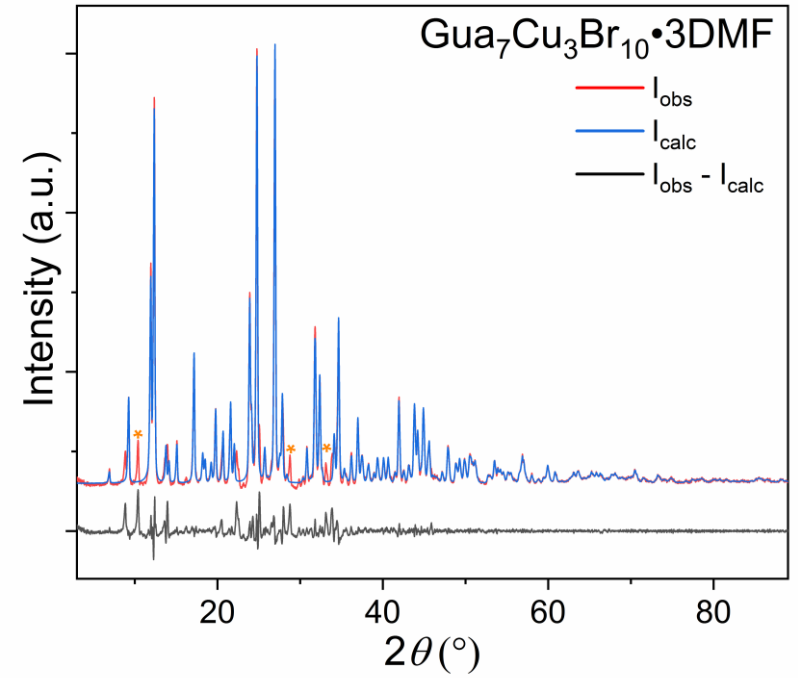


Figure S5. Comparison of measured PXRD pattern for $Gua_7Cu_3Br_{10}$·3DMF with calculated pattern produced by decomposition fitting to SCXRD-generated crystallographic information file (CIF) parameters. Starred peaks are attributed to degradation products of $Gua_7Cu_3Br_{10}$·3DMF in the presence of air.

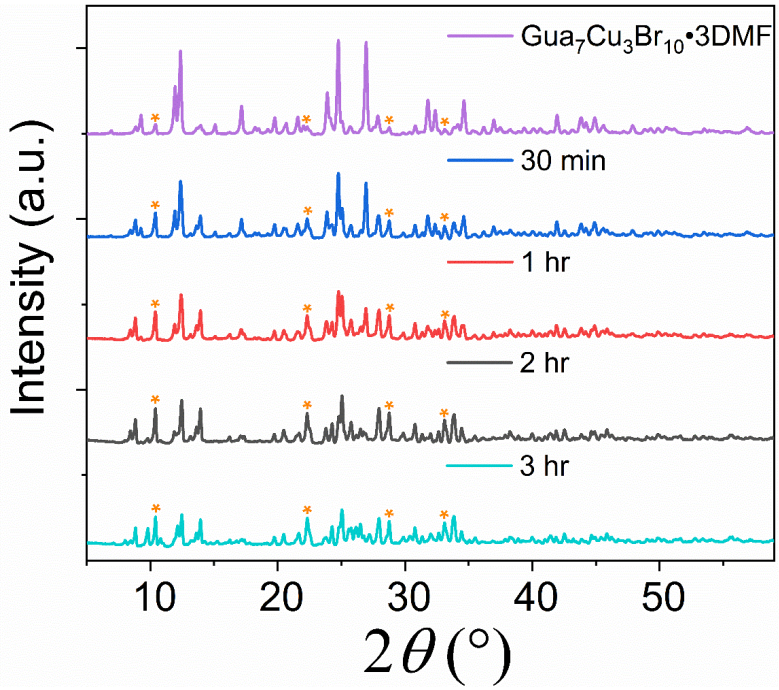


Figure S6. PXRD patterns for $Gua_7Cu_3Br_{10}$·3DMF taken over the course of three hours, with starred peaks assigned to degradation products resulting from exposure to air and moisture.

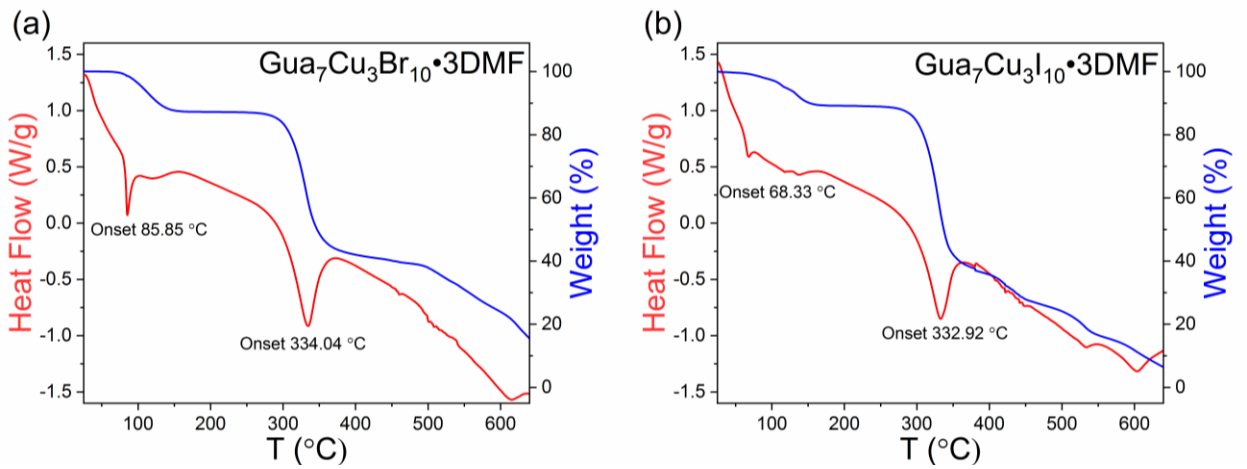


Figure S7. Thermogravimetric analysis (blue) and differential scanning calorimetry (red) plots for (a) $Gua_7Cu_3Br_{10}$·3DMF and (b) $Gua_7Cu_3I_{10}$·3DMF.

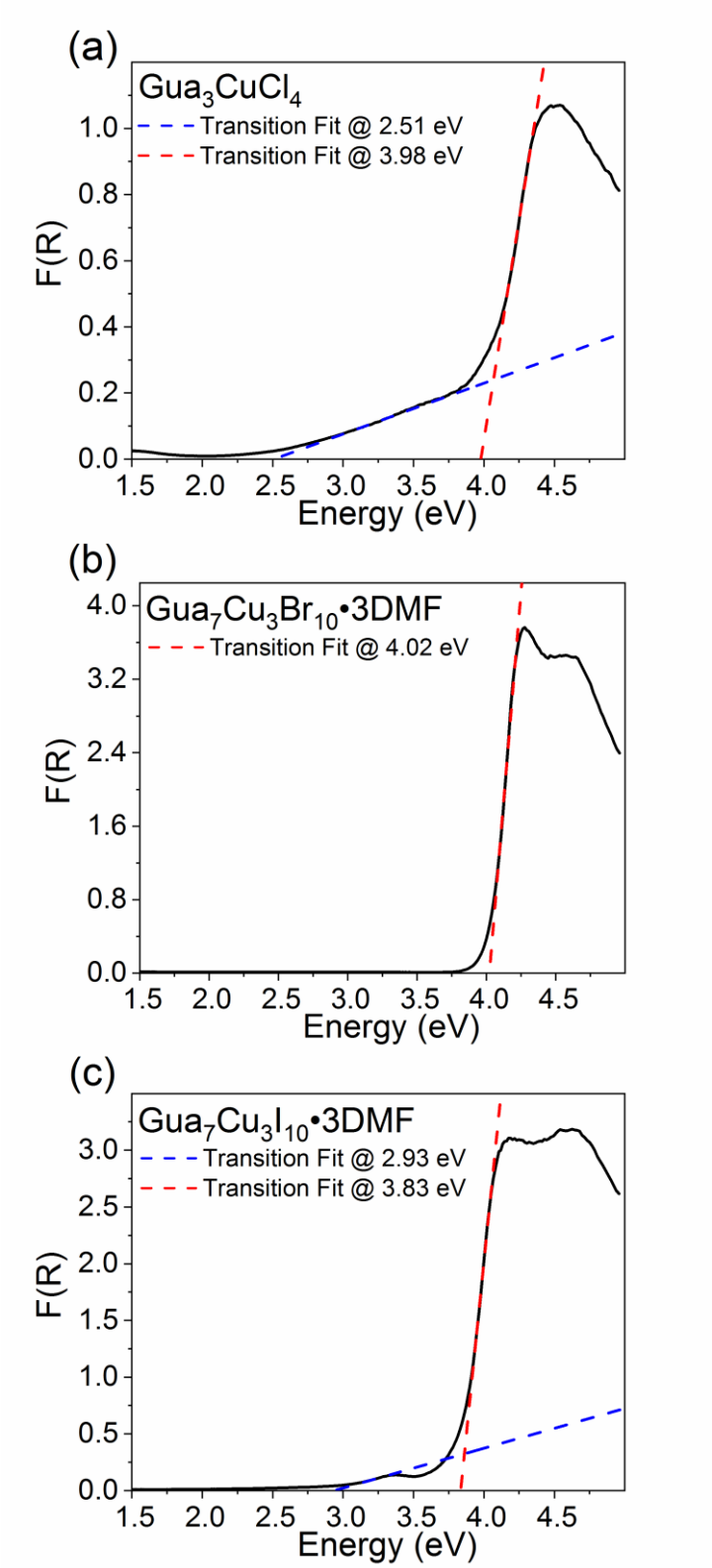


Figure S8. Pseudo-absorbance spectra made using the Kubelka-Munk transform on diffuse reflectance data for (a) Gua_3CuCl_4, (b) $Gua_7Cu_3Br_{10}\cdot 3DMF$, and (c) $Gua_7Cu_3I_{10}\cdot 3DMF$.

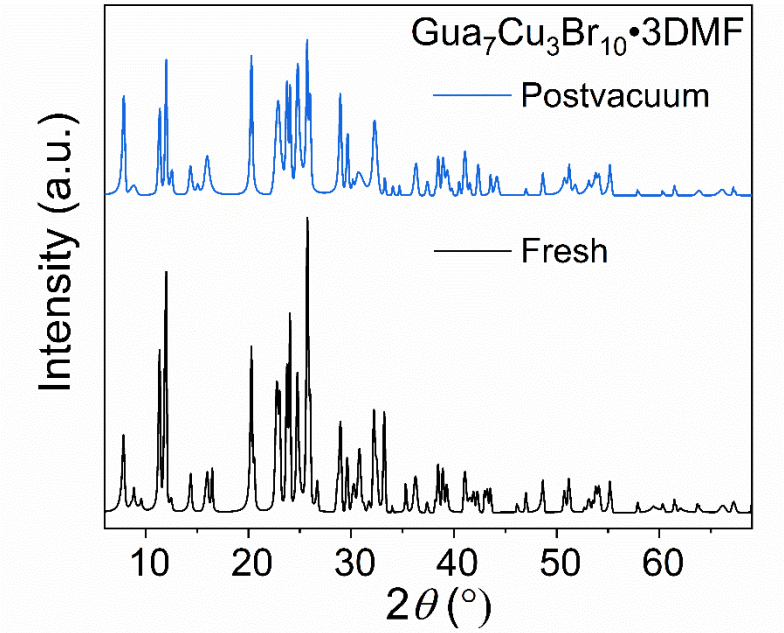


Figure S9. PXRD comparison between a fresh sample of $Gua_7Cu_3Br_{10}$·3DMF and the same sample after 4 days under vacuum.

Table S6. R1-R15 values for $Gua_7Cu_3I_{10}$·3DMF emission at 315 and 345 nm excitation wavelengths.

R Value	λ_{ex} **= 315 nm**	λ_{ex} **= 345 nm**
R1	93	97
R2	95	98
R3	95	98
R4	94	97
R5	94	97
R6	93	97
R7	96	98
R8	92	95
R9	73	86
R10	87	95
R11	92	97
R12	89	96
R13	94	97
R14	97	99
R15	92	96

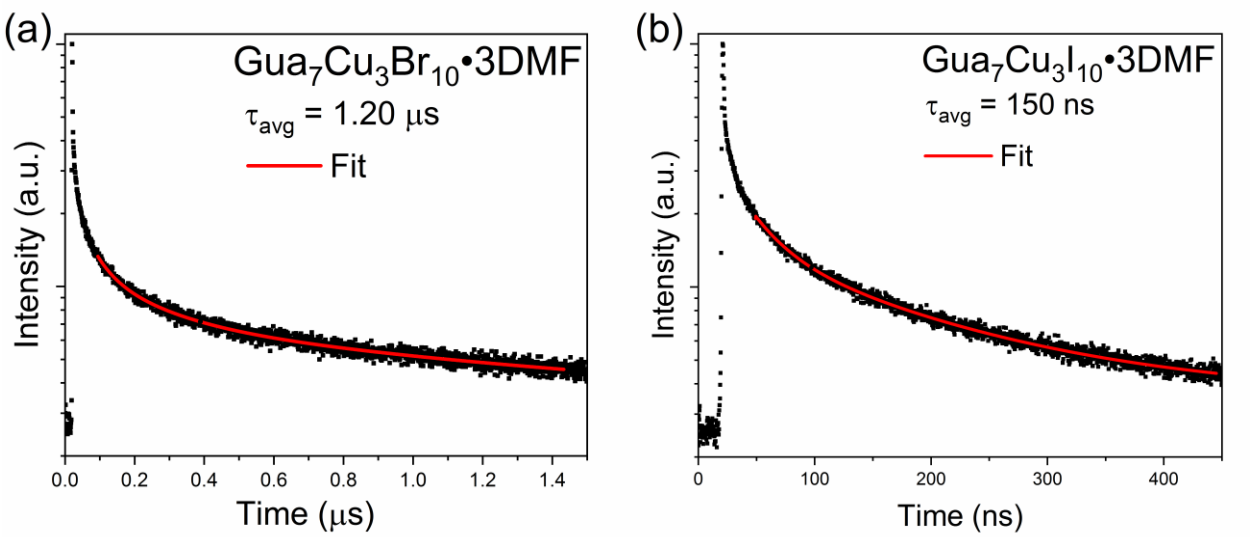


Figure S10. Time-resolved photoluminescence data (black) with fitting curves (red) for (a) $Gua_7Cu_3Br_{10}\cdot 3DMF$ and (b) $Gua_7Cu_3I_{10}\cdot 3DMF$.

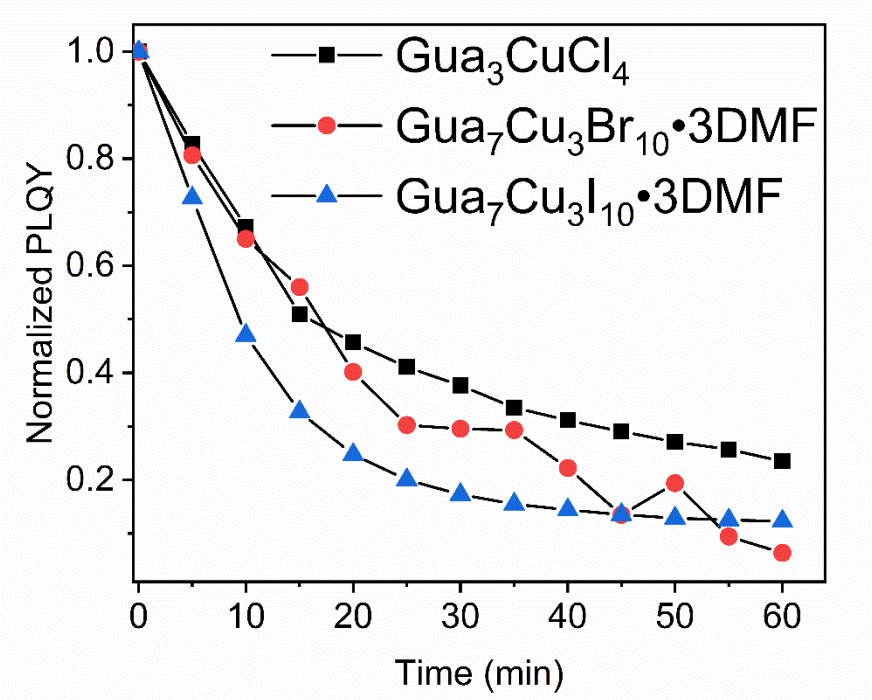


Figure S11. Photostability comparison plot for (black) Gua_3CuCl_4, (red) $Gua_7Cu_3Br_{10}\cdot 3DMF$, and (blue) $Gua_7Cu_3I_{10}\cdot 3DMF$.